A study of the calibration of wire positions for the BESⅢ drift chamber using physics data without magnetic field*

WU Ling-Hui(伍灵慧)[1)]   WANG Yi-Fang(王贻芳)   CHEN Yuan-Bo(陈元柏)

LIU Jian-Bei(刘建北)   LIU Rong-Guang(刘荣光)   MA Xiao-Yan(马骁妍)

(Institute of High Energy Physics, CAS, Beijing 100049, China)

Abstract   A method to determine precisely three-dimensional wire positions in the BESⅢ drift chamber using physics events is introduced. In part the proposed technique takes advantage of the possibility that the magnetic field can be turned off, thereby providing a huge sample of straight tracks for which effects due to multiple scattering, energy loss and non-uniformity of the magnetic field are minimized during the calibration process. A toy Monte Carlo study is performed to demonstrate the viability of the method. As a result of the calibration process, the rms of the distribution of wire position deviation is reduced from 35 μm to 10 μm.

Key words   BESⅢ, drift chamber, wire position, calibration

PACS   29.40.Gx, 29.85.Fj

1   Introduction

The upgraded Beijing Electron Positron Collider (BEPCⅡ) is a high luminosity, multi-bunch collider with a design peak luminosity of 10^{33} cm$^{-2}\cdot$s^{-1} at 1.89 GeV. The BESⅢ detector which will operate at BEPCⅡ, is designed for high-precision measurements and new physics searches in this energy region. Such goals require that exclusive final states from the e$^+$e$^-$ collision be reconstructed efficiently and with high resolution. This places stringent demands on the performance of the central tracking detector. The BESⅢ drift chamber, operating in a 1 T magnetic field, is required to provide maximal solid angle coverage, good spatial resolution (130 μm), good momentum resolution (0.5%@1 GeV/c), efficient tracking down to 50 MeV/c and comparative dE/dx resolution (6%—7%)[1]. Results of a beam test of a prototype chamber validate the physics capabilities of the BESⅢ drift chamber[2].

In order to meet these requirements, a small-cell geometry and low-mass materials are chosen. The drift cell is almost square and the ratio of the number of field wires to that of sense wires is nearly 3.

There are 43 sense layers in total. The average half-cell size is 6 mm for the inner most 8 layers and 8 mm for the other 35 layers. Aluminum field wires are used and the working gas is He/C$_3$H$_8$ (60/40).

Uncertainties of wire positions are contributors to the spatial resolution of the drift chamber. Errors in the sense wire locations contribute directly, while errors of field wire positions contribute indirectly by producing cell-to-cell variations in the time-to-distance relationship[3]. In the BESⅢ drift chamber, the uncertainties come mainly from the hole location, the position error of the feedthrough in the hole, concentricity of the feedthrough and the position error of the wire in the pin. Table 1 shows the estimated position error from each of these items. In addition, variations in the wire tension also contribute to the spatial resolution. The wire tensions were required to be uniform to within ±5% during the construction of the BESⅢ drift chamber.

In the calibration of the BESⅡ drift chamber, only the average deviation perpendicular to radial direction of the entire wire was corrected, while the position difference between the two endpoints of each wire was not considered. In the BESⅢ drift chamber,

No. 4

WU Ling-Hui et al: A study of the calibration of wire positions
for the BESIII drift chamber using physics data without magnetic field

265

we expect to realize a more precise determination of wire positions by making use of the variation of residuals in z direction, using the collision events accumulated without a magnetic field. In that case, the track trajectories will be straight lines rather than helices. The track fitting will be simpler and more precise due to the minimization of the effects from dE/dx, multiple scattering and the non-uniformity of the magnetic field, which is typically a few percent. In order to achieve this, a large sample of tracks will be needed, which can be obtained at the high luminosity BEPCII.

Table 1. Estimated position errors of the wire.

item	rms/μm	
	sense wire	field wire
hole location	25.0	25.0
feedthrough in hole	6.3	6.3
crimp pin hole	12.5	12.5
wire in pin hole	31.3	10.0
total rms	42.4	30.3

This paper introduces a method of wire position calibration and the results of a Monte Carlo study of its viability.

2   Description of the wire

Wires in the drift chamber are subject to gravitational and electrostatic forces that are balanced by restoring forces provided by the wire tension[4] (see Fig. 1). The equation describing the wire stability can be written as follows[5]:

$$F_{\text{restoring}} + F_{\text{elec}} + F_{\text{gravity}} = 0 . \tag{1}$$
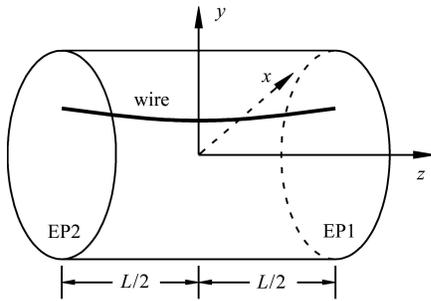

Fig. 1.   View of the drift chamber and the wire (EP means the endplate).

Simulation shows that the displacement of the wire caused by the electrostatic force is less than 10 μm, so it is ignored in our study in which case Eq. (1) can be written as:

$$T\frac{d^2y}{dz^2} + \rho g = 0 , \tag{2}$$

where T is the mechanical tension per unit length, ρ is the linear density of the wire and g is the gravitational acceleration. The first term on the left is the restoring force per unit length, while the second term is the gravitational force per unit length.

With the boundary condition,

$$\begin{cases} y(z=-L/2)=y_1 \\ y(z=L/2)=y_2 \end{cases} , \tag{3}$$

where L is the length of the wire, the solution of Eq. (2) is:

$$y = az^2 + \frac{y_2 - y_1}{L}z - \frac{aL^2}{4} + \frac{y_1 + y_2}{2} , \tag{4}$$

where $a = -\dfrac{\rho g}{2T}$. For an ideal axial wire, y_1 is equal to y_2, so the gravitational sag at $z=0$ is $\dfrac{\rho g}{8T}L^2$. For the stereo wire, Eq. (4) must be transformed to the wire plane because it is not parallel to z.

Equation (4) is only for describing a wire in y-z plane. For an arbitrary wire in the chamber, 5 independent parameters are needed. We choose x_{EP1}, y_{EP1}, x_{EP2}, y_{EP2} and T, where the first 4 parameters are the coordinates of each endpoint of the wire in x-y plane, respectively, and T is the tension of the wire. When Eq. (4) is extended to 3 dimensions, the wire can be described as follows:

$$\begin{cases} x = (z - z_{\text{EP1}}) \cdot \tan\alpha + x_{\text{EP1}} \\ y = \dfrac{az^2}{\cos^2\beta} + (y_{\text{EP2}} - y_{\text{EP1}}) \cdot \dfrac{z}{L_{\text{w}} \cdot \cos\beta} + \\ \quad \dfrac{1}{2}(y_{\text{EP2}} + y_{\text{EP1}}) - \dfrac{aL_{\text{w}}^2}{4} \end{cases} , \tag{5}$$

where β is the angle between z axis and the projection of the wire in x-z plane, and L_{w} is the distance between the two endplates.

3   Method of wire position correction

The residual is defined as

$$r = d_{\text{meas}} - d_{\text{track}} , \tag{6}$$

where r is the residual, d_{meas} is the measured distance, d_{track} is the distance from the fitted track to the sense wire. The sign of d_{meas} and d_{track} is "+" for the track in the right of the sense wire and "−" in the left. The least square method is used in the track fitting where the χ^2 is defined as:

$$\chi^2 = \sum_{i=1}^{N} \frac{r_i^2}{\sigma_i^2} , \tag{7}$$

where N is the number of hits, and σ_i is the inverse-weight of the i-th hit. The offset of the wire $\Delta d_{\text{wire}}(z)$

can be obtained from the residual distribution:

$$\Delta d_{\text{wire}}(z) = -\frac{\overline{r_{\text{L}}(z)} + \overline{r_{\text{R}}(z)}}{2}, \qquad (8)$$

where $\overline{r_{\text{L}}(z)}$ is the mean of the residual distribution on the left of the sense wire at z, and $\overline{r_{\text{R}}(z)}$ is the corresponding quantity on the right of the sense wire. Since all the tracks are straight and radial, only the offset of the wire in the direction perpendicular to the track can be obtained. $\Delta d_{\text{wire}}(z)$ can be decomposed into $\Delta x_{\text{wire}}(z)$ and $\Delta y_{\text{wire}}(z)$ which can be written as (see Fig. 2):

$$\begin{cases} \Delta x_{\text{wire}} = -\Delta d_{\text{wire}} \cdot \sin \varphi_{\text{wire}} \\ \Delta y_{\text{wire}} = \Delta d_{\text{wire}} \cdot \cos \varphi_{\text{wire}} \end{cases}. \qquad (9)$$
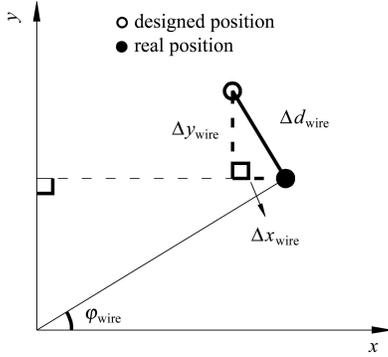

Fig. 2.　View from x-y plane.

Wire position calibrations are performed wire-by-wire based on Eqs. (8) and (9). The wire is divided into N intervals in the z dimension. The offset of the center in each interval is obtained from Eqs. (8) and (9), and a series of corrected points along the wire are obtained by adding the offsets to the calculated positions. A fit to a parabola, as described in Eq. (5) to these corrected points, using a least square method with χ^2 defined as:

$$\chi^2 = \sum_{i=1}^{N} \frac{(x_{\text{cor}}^{(i)} - x_{\text{fit}}^{(i)})^2 + (y_{\text{cor}}^{(i)} - y_{\text{fit}}^{(i)})^2}{\sigma_i^2}, \qquad (10)$$

provides a new set of parameters for the wire. Here $x_{\text{cor}}^{(i)}$ and $y_{\text{cor}}^{(i)}$ are the corrected positions of the center of the i-th interval, and $x_{\text{fit}}^{(i)}$ and $y_{\text{fit}}^{(i)}$ are the positions of the wire in the center of the i-th interval, which are functions of the 5 wire parameters, and σ_i is the inverse-weight of the i-th point.

4　A toy Monte Carlo study

A toy Monte Carlo simulation has been performed to study the validity of the correction method. The nominal wire positions are smeared according to Table 1. The wire tension are also smeared to produce a $(-5\%, 5\%)$ uniform distribution. Generated events are simulated based on the smeared wire positions and tensions; all the generated tracks are straight lines from the center of the drift chamber. During the track fitting, wire position values are corrected by means of self-tracking with iterations.

Figure 3 shows the results of the correction of the wire displacement in the dimension perpendicular to tracks. We can see that the estimated wire positions are very close to the smeared ones, and the rms of deviations is reduced from 35 μm to 10 μm after the calibration. Wire displacements in the direction perpendicular to tracks are well corrected because the residual is the most sensitive to the wire displacement in this direction.

In contrast to the above case, displacements in the dimension parallel to tracks can not be corrected (see Fig. 4). In this dimension, the wire displacement has little impact on the residual and track fitting, and so corrections are difficult. In general, wire displacements in the radial direction can not be corrected using data without a magnetic field. For this we can use low momentum tracks with a magnetic field.
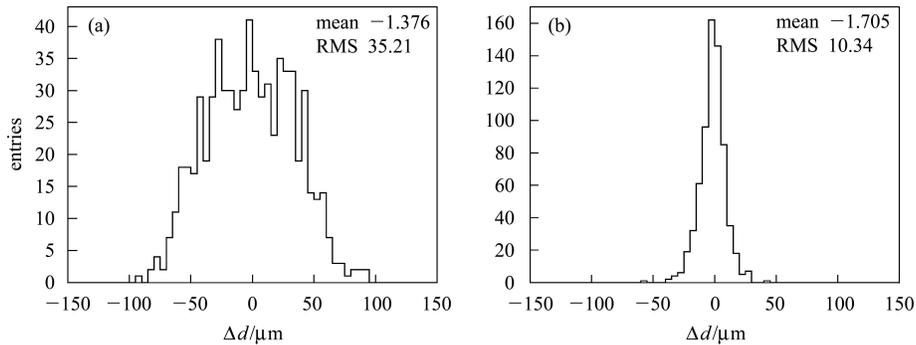

Fig. 3.　The results of the calibration of the wire displacement in the direction perpendicular to tracks. (a) Distribution of deviations of smeared wire positions from the design values; (b) Distribution of deviations of the corrected values from the smeared ones.
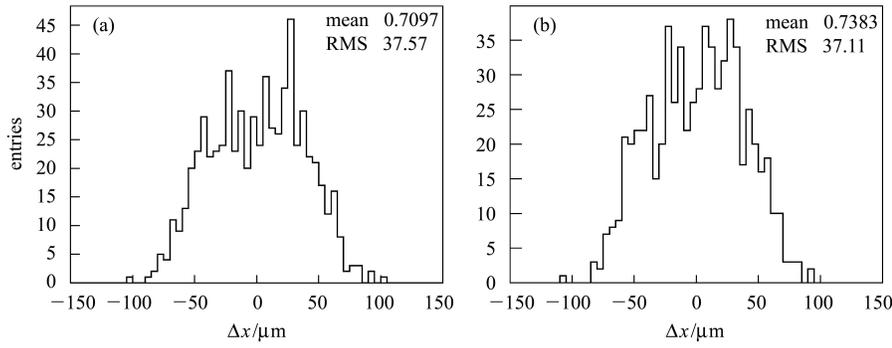
Fig. 4. The results of the calibration of the wire displacement in the direction parallel to tracks. (a) Distribution of deviations of smeared wire positions from the designed values; (b) Distribution of deviations of the corrected values from the smeared ones.

Figure 5 shows the result of wire tension corrections. The deviations of the tension are only slightly changed. This is because in the BESIII drift chamber, the variation of the wire sag is less than 10 μm for tension variations that are not more than 5%. Tension variations at this level have little impact to the track fit and the spatial resolution, and corrections are not necessary if the deviation of tensions is, in fact, less than 5%.
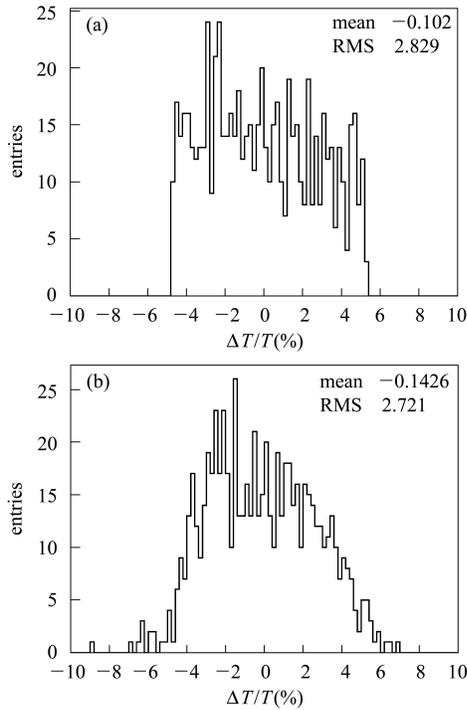

Fig. 5. Distribution of the deviation of T, (a) before and (b) after the calibration.

Figure 6 shows the residuals for a wire as a function of z. Different deviations between the two endpoints of the wire result in the variation of the residual in z direction (shown in Fig. 6(a)). After the correction, this variation nearly disappears.
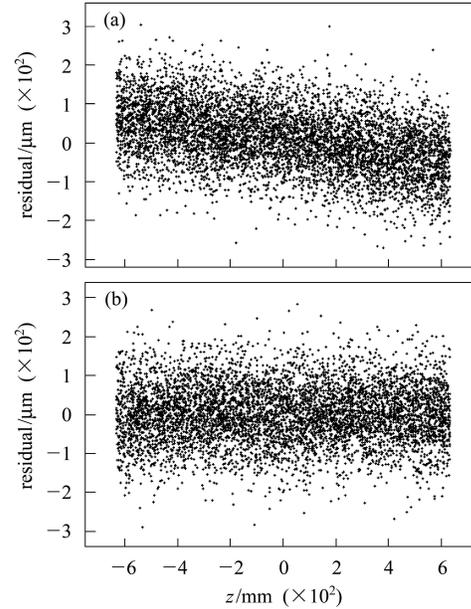

Fig. 6. Residual as a function of z, (a) before and (b) after the correction.

Figure 7 shows the variation of the spatial resolution with the drift distance before and after calibration respectively. It can be seen that there are bigger changes to the spatial resolution in the middle region between the sense wire and the field wire than that for the regions near the sense wire or field wire. In this middle region, the spatial resolution is improved by 7 μm, where the intrinsic resolution is 50—60 μm.
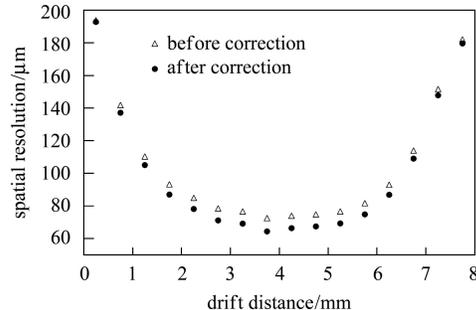

Fig. 7. Impact to the spatial resolution.

5   Requirement for the data acquisition

If the same calibration is performed wire-by-wire using dimuon events, a huge data sample would be needed. Since the data without magnetic field can only be used for the determination of wire positions, it is impossible to spend too much time on it. Fortunately, the high luminosity of BEPCII provides the possibility for this. In a Monte Carlo study, at least 20 000 events are needed for correcting each sense wire, and, since there are 288 cells in the outmost layer of the BESIII drift chamber, we need a sample of nearly 3 000 000 $J/\psi \to \mu^+\mu^-$ to perform this calibration. From the cross section[6],

$$\frac{\mathrm{d}\sigma}{\mathrm{d}\Omega} = \frac{\alpha^2}{4s}(1+\cos^2\Theta)\{1+|A_{\mathrm{R}}^{\varepsilon\mu}|^2 - 2\mathrm{Re}(A_{\mathrm{R}}^{\varepsilon\mu})\}, \quad (11)$$

taking into account of the angular distribution, nearly twice the dimuon events may really be required. The event rate will be 2000 Hz at the J/ψ resonance[1] and the branching fraction is (PDG 2004):

$$Br(J/\psi \to \mu^+\mu^-) = (5.88 \pm 0.10)\%. \quad (12)$$

So nearly 100 million J/ψ events will be required, which would take about 14 hours of data taking at the design luminosity $(0.6\times10^{33}\ \mathrm{cm}^{-2}{\cdot}\mathrm{s}^{-1})$. We believe that it meets our need.

6   Conclusion and prospects

In this method we make use of the variation of residuals along the wire and achieve a three-dimensional calibration of wire positions in the BESIII drift chamber. The result of a toy Monte Carlo study shows that the method is effective for precisely determining the displacement of the wires perpendicular to the radial direction, which has the main impact to the track fitting. The rms of the deviation distribution is improved to 10 μm from 35 μm after the calibration. The spatial resolution is also improved. It can be concluded that the correction of the wire sag is difficult when the non-uniformity of tensions is less than 5% which is guaranteed during the construction of the chamber, since it has little impact to the track fit and the spatial resolution. Further study is required to taking into account the effects of multiple scattering and energy loss in BESIII Offline Software System[7].

References

1   BESIII Collaboration. BESIII Preliminary Design Report, 2004
2   LIU J B et al. Nucl. Instrum. Methods A, 2006, **557**: 436
3   Hearty C. BaBar-TNDC-95-12, Oct.15, 1995
4   Sudou S et al. Nucl. Instrum. Methods A, 1996, **383**: 391
5   Va'vra J. Calculation of Two-Dimensional Electrostatic Field in a Drift Cell: SLAC Detector Techniques Lectures. 1998
6   Köpke L, Wermes N. J/ψ Decays. CERN-EP/88-93
7   LI Wei-Dong, LIU Huai-Min et al. The Offline Software for the BESIII Experiment. Proceeding of CHEP06, Mumbai, 2006